1949

The design, construction, and installation of a test model for the study of flow in nozzles

Boettcher, Robert Richard; Gunnels, Charles W.; Rodgers, Edward A.

http://hdl.handle.net/10945/6358

THE DESIGN, CONSTRUCTION AND INSTALLATION OF A TEST MODEL FOR THE STUDY OF FLOW IN NOZZLES

ROBERT R. BOETTCHER
CHARLES W. GUNNELS, JR.
EDWARD A. RODGERS

THE DESIGN, CONSTRUCTION, AND

INSTALLATION OF A TEST MODEL FOR THE

STUDY OF FLOW IN NOZZLES

by

Robert R. Boettcher
B.S. in E.E., U.S. Naval Academy, 1940

Charles W. Gummels, Jr.
B.S. in E.E., U.S. Naval Academy, 1941

Edward B. Rodgers
B.S. in E.E., U.S. Naval Academy, 1940

Submitted in partial fulfillment of the requirements for the degree of Master of Science at the Massachusetts Institute of Technology

1949

ACKNOWLEDGEMENTS

The authors wish to express their deep appreciation to Mr. Hans Kraft of the General Electric Company for his direction and guidance; to Professor E. S. Taylor for his close supervision; and to Professor S. Ober, Mr. F. Lustwerk, Mr. L. DeFrate and the Gas Turbine Laboratory personnel for their generous assistance upon many occasions.

Cambridge, Massachusetts.

20 May, 194[illegible].

Professor Joseph [illegible]. Newell,
Secretary of the Faculty,
Massachusetts Institute of Technology,
Cambridge, Massachusetts.

Dear Sir:

In partial fulfillment of the requirements for the degree of Master of Science in Aeronautical Engineering, we hereby submit a thesis entitled, "The Design, Construction, and Installation of a Test Model for the Study of Flow in Nozzles."

Respectfully,

TABLE OF CONTENTS

SUMMARY

The object of this project was to design, construct, and install in the Gas Turbine Laboratory a test model for the study of flow in nozzles. This object was achieved and the model is now ready for test work.

This thesis includes a discussion of problems solved in the design, a complete description of the model, and a discussion of procedures to be used and results to be expected when the apparatus is used in tests.

I INTRODUCTION

Ia. Statement of the Problem. The object of this thesis was to design, construct, install, and test if possible, in the limited time available, a nozzle cascade model in the Variable Density Wind Tunnel in the Gas Turbine Laboratory.

The basic nozzle cascade was furnished by the General Electric Company; the blade sections are double scale reproductions of some in current use in large turbines. Around this basic blade a model was designed to incorporate the necessary features for conducting a complete pressure survey through the nozzle passage and in the exit plane of the cascade. The model is also equipped with optical flats mounted on each side wall for use with the interferometer in making a survey of density gradients and general flow pattern to study the boundary layer.

The installation will permit tests to be made at either a constant Mach Number or a constant Reynolds' Number, and the effects of each can be isolated. It is expected that over-all Mach Numbers from 0.3 to 0.95 and Reynolds' Numbers from 10,000 to 300,000 will be obtained. This should give a number of interferometer band shifts ranging from 1 to 50.

The design was completed under the direction and with the assistance of Mr. Hans Kraft of the General Electric Company and Professor E. S. Taylor of the Aeronautical Engineering Department. The General Electric Company manufactured the model. The necessary large piping for the wind tunnel was

manufactured by a local contractor, and the optical flats were furnished by Perkin-Elmer Corporation of Glenbrook, Connecticut. The installation was completed with the able assistance of the Gas Turbine Laboratory personnel.

Due to the delays and difficulties encountered in the manufacture and installation of the various components time did not permit more than part of the preliminary testing of the model. The installation was checked thoroughly for leaks and for proper functioning of all components. The installation is now ready for the tests for which it was designed, and preliminary runs indicate that the design is satisfactory.

Ib. Historical Background. A considerable amount of testing has been done by the General Electric Company on the blades used in this cascade and some curious flow effects have been noted. Losses in efficiency accompanied these effects. The facilities available at the time did not allow a complete separation of the effects of Mach Number and Reynolds' Number. In order to investigate the problem more thoroughly, it was suggested that an Interferometer be used in connection with a variable density wind tunnel and the Massachusetts Institute of Technology was asked to continue the study.

Ic. Proposed Scope of Investigation. It was intended that tests be conducted for the eventual determination of the

nozzle efficiencies at several values of Mach Number and Reynolds' Number, indicating their relative effects. In addition, the interferometer was to be used to supplement the above information and to permit a study of the nozzle flow with particular regard for the boundary layer.

II Design and Description of Test Model

IIa. Design of Model. The first step taken toward the design of the model was the construction of Figure 'A'. A characteristic length of 1/2 inch, based on the width of the nozzle throats, was used in the computation of Reynolds' Number for various pressure ratios. Using the equation (see Appendix) given by Gilbert H. Edelman in his thesis entitled "The Design Development and Testing of Two-Dimensional Sharp Cornered Supersonic Nozzles" the number of expected interferogram band shifts were computed for various pressure ratios and pressures. These results were plotted as shown in Figure 'A' and provide a picture of the areas to be covered.

It was required by the sponsor, General Electric Company, that the cascade section be composed of blades supplied by them. The nozzle throats were also established as 1/2 inch wide. Due to space limitations in the throat of the interferometer and also due to the desirability of decreasing as much as possible the side wall effects by using a large model width, it was decided that a 6-inch blade length was the best compromise. It was also desirable to include as many passages as possible to nullify end wall effects, but the available air supply limited this dimension. An odd number of passages was necessary to insure equal end wall effects on the middle

passage which was to be subjected to the investigation. Using the basic equation shown on the chart, Figure '[illegible]' was constructed showing the compressor capabilities; data for this curve was supplied by the Gas Turbine Laboratory. With this chart it was decided that 7 passages with a total throat area of 21 square inches would be used.

Provision had to be made for mounting the optical flats through which the interferometer exposures would be made. The sponsor desired a large field of view which was to include a complete nozzle passage. After due consideration of mounting problems, area coverage, pressure tap leads, and blade supports the windows were located as shown in Figures 'H' and 'I'. Holes were drilled in the windows to admit supports for the blades, but clearances are provided and no side loads are taken by the glass.

It was important that provision be made for taking a pressure traverse across the nozzle exits. This was accomplished by designing the airtight slide and sliding tube assembly shown in Figure 'K'. This assembly permits a traverse to be made covering the whole cascade exit area in a plane 0.3 inches behind the blade trailing edges. The sponsor designated the location of the static pressure orifices in the sides of the middle nozzle. These are shown in Figures '[illegible]' through '[illegible]' and Figures '[illegible]', '[illegible]', and '[illegible]'. The pressure tubes are carried out through the

sides of the model, through the blade supports.

The blueprints from which the model was manufactured are on file in the Gas Turbine Laboratory office.

IIb. Description of Model. The model is shown complete in Figures 'H' through 'M'. The model casing is made of 3/8 inch steel plate and is almost entirely bolted together for ease in disassembly. All meeting surfaces have been ground and the necessity for using sealant in these joints is obviated. The interior surface of the casing has a ground finish and great care has been taken to make the entire model a precision instrument.

The basic conformation includes the two side plates which provide a location for the glass windows. These side plates may be moved one blade spacing by adding or removing the spacer shown immediately ahead of the exit flange in Figure 'M'. This relocation of the sides permits an interferometer study of the nozzle following the one of primary interest. In addition, an extra side has been provided for the right side of the model to permit the required exit plane traverse to be made. This side is shown in Figure 'K'.

The optical flats which give a clear area of 6 inch diameter are located on either side of the nozzles to be studied. These flats were ground to the same degree of accuracy, 1/20 of a wavelength of violet light as were those used in

the interferometer. Two holes for the blade supports are located in each window. These windows are so mounted, seated in lead, that no interruption of flow will occur at their edges, i.e. the interior wall is perfectly smooth.

The blade supports projecting through the windows are further supported by arms projecting from the window mounting rings. This is disadvantageous because it decreases the field of view but no other completely satisfactory solution could be devised. The blade supports are not in contact with the glass and the windows therefore support no load with the exception of the air load due to their exposed areas which they will carry with no recognizable distortion.

Static pressure orifices are located in both blades bordering the middle nozzle passage and have been discussed in the preceding subsection.

Figure 'K' shows the third side in place and also shows how the pressure traverse is made. A keyed slide has been incorporated into this side plate and this slide in turn holds a sliding tube which may also be rotated 360°. The impact head is fixed to the end of this tube. The slide permits travel in the direction of flow, the tube permits travel across the cascade section, and the rotation of the tube permits the determination of flow direction.

An access plate is located in the top of the model. This plate is intended to permit access to the interior of the model without disturbing the critical mounting of the optical flats.

III Installation

The model was designed such that it would replace an elbow in the 24 inch steel pipe forming the Variable Density Wind Tunnel circuit. Short lengths of pipe were used as spacers to raise the model to an average height of eye. Due to the limited interferometer throat width it was found necessary to construct a rectangular section to replace the large pipe directly under the model. This required a decrease in flow area and possibly will have a deleterious effect upon the boundary layer in the model inlet. The installation is shown in Figures 'G' and 'H'.

The air screen shown in Figure 'F' was designed to stop all rotational flow and to break up all large scale turbulence in the flow before it reached the model. The screen is composed of approximately 50 aluminum tubes, 2 1/2 inch O.D. and 25 inches long. A 12 mesh screen covers both the inlet and outlet of the air screen. A large mesh expanded metal screen is used at each end to insure that the tubes will remain in place. The assembly is installed in the tunnel circuit approximately 3 1/2 feet ahead of the model entrance, the flange on the air screen being clamped between the two pipe flange faces shown close to the floor in Figures 'H' and 'G'.

A sharp edged orifice with a pressure tap on each side is located in the tunnel circuit, permitting an accurate determination of mass flow to be made. This orifice will not effect flow in the model.

A thermocouple is installed in the large pipe leading into the test assembly. With the installation of a total pressure tube in the same general location the complete determination of entrance conditions may be made. A static pressure orifice located in the diffuser section of the model will, in conjunction with the total pressure tube ahead, permit the calculation of the 'overall Mach Number' of the flow.

All pressure orifices and taps were connected to a bank of mercury manometers by means of plastic 'stripper' tubing. A total of [illegible] manometers is required for the necessary pressure readings, and others will be needed for atmospheric bases.

IV. Discussion

Using the variable density wind tunnel and the interferometer a steady state, compressible, two-dimensional flow will be examined. Flow through the model is considered to vary directly as temperature and the effects of boundary layer shock, i.e., roughness of the model, are considered negligible.

In order to analyze the results most effectively it is desirable to make the test run in such a manner that the effect of Mach Number can be distinguished from that of Reynolds' Number. To do this, Mach Number will be held constant on a given run and Reynolds' Number will be varied.

The Mach Number used is the 'over-all' or theoretical Mach Number at the exit which is computed from the average static pressure in the exit passage and the total pressure ahead of the nozzle. This is an isentropically computed Mach Number when the loss in total pressure in the nozzle due to friction is neglected. By neglecting this loss which varies with Reynolds' Number, slight variations in the actual Mach Number are permitted even when the pressure ratio is held constant. These are considered small and are neglected because the variation in nozzle efficiency is not large. The overall Mach Number is to vary from 0.7 to 0.95 approximately.

The velocity distribution in the actual flow through a nozzle passage will vary across any section perpendicular

to the average flow direction. This means that local Mach Numbers may exist which are larger than the average Mach Number at that nozzle section. Therefore, one of the first things that should be done is to make a survey by means of the static pressure holes at various pressure ratios to determine the local Mach Numbers along the blade surface. When the local Mach Number reaches a value of 1.1 or 1.2 this should be considered the limiting pressure ratio. Any further increase in the local Mach Number would mean a comparatively serious loss in nozzle efficiency due to shocks occurring in the flow.

The other variable, Reynolds' Number, is varied by changing the static pressure in the tunnel. The temperature at the nozzle entrance is considered constant and is maintained so with the help of the thermocouple, upstream from the model, and cooler at the compressor. The characteristic length is the nozzle throat which in this nozzle is 0.3 inches.

One of the principal objects of this investigation is to show the effect on nozzle efficiency of the two variables, Reynolds' Number and Mach Number. Since the nozzle is considered adiabatic the loss in efficiency is due to friction forces between the fluid and the contact surfaces, and also friction in the fluid itself. Efficiency is calculated from the loss in total pressure through the nozzle, where this loss represents a transfer of kinetic energy to heat energy as a result of friction.

Thinking of an actual test run at a given Mach Number and Reynolds' Number and then considering the values of impact pressure recorded on the traverse at the exit, the total pressures vary over the nozzle exit area. The loss in total pressure will be largest near the solid surfaces which make up the nozzles' boundaries, where, of course, the boundary layers occur. The total pressure for the flow in the nozzle's central core will show a nearly isentropic change with the loss in total pressure increasing rapidly as we approach a solid surface. In order to compute 'nozzle efficiency' we must integrate all the various efficiencies occurring in one nozzle passage, and this integrated efficiency then becomes the 'nozzle efficiency' for that particular run.

As indicated, the efficiency in the nozzle very nearly approaches the isentropic case except near the boundary layers. Therefore it becomes important to determine from test data as much about the boundary layer as possible and in particular to know the separate effects of Mach Number and Reynolds' Number on the transition from laminar to turbulent flow in the boundary layer. From literature, on the subject of transition, it can be said that transition occurs when the Reynolds' Number reaches a critical value. The actual value of the critical Reynolds' Number depends on the turbulence in the main stream, roughness of the surface, shape of the leading edge, etc. The pressure gradient found with an accelerating flow retards transition. Finally, centrifugal force seems to have a strong influence on when

transition occurs. In flow around a curved path such as that presented in this model transition to turbulent flow should occur on the concave side first. A brief explanation of this centers about the fact that the particles on the outside of the boundary layer are moving faster and consequently have more centrifugal force acting on them than the particles in a layer closer to the concave surface. Thus, the particles on the outside tend to be thrown into the wall thereby disturbing the flow, tending to set up eddies, and establishing turbulent flow at fairly low Reynolds' numbers. On the convex side more or less the opposite is true, since particles with too much centrifugal force are thrown into the main stream and do not disturb the laminar layer next to the wall.

According to S. Goldstein in his recent book on Fluid Dynamics the shearing stress at the surface of a flat plate decreases downstream in a fully laminar region; it also decreases in the same way in a fully turbulent region, but in the region of transition from laminar to turbulent flow the shearing stress increases until the transition is complete. Also it should be noted that transition does not occur instantaneously but rather requires a finite distance along the body's surface. In general this same information is available in the well known curves of friction or friction drag of a body moving through a fluid medium plotted against Reynolds' Number. These latter curves show friction decreasing

as Reynolds' Number increases in both the laminar and turbulent regions, but the turbulent curve lies above the laminar one, so that in order to get to it from the laminar one the friction must increase during the period of transition.

From this knowledge of the Boundary Layer and Friction in the boundary layer it is possible to indicate the type of curve which would be expected if one plots nozzle efficiency versus the logarithm of Reynolds' Number. This curve is as follows:

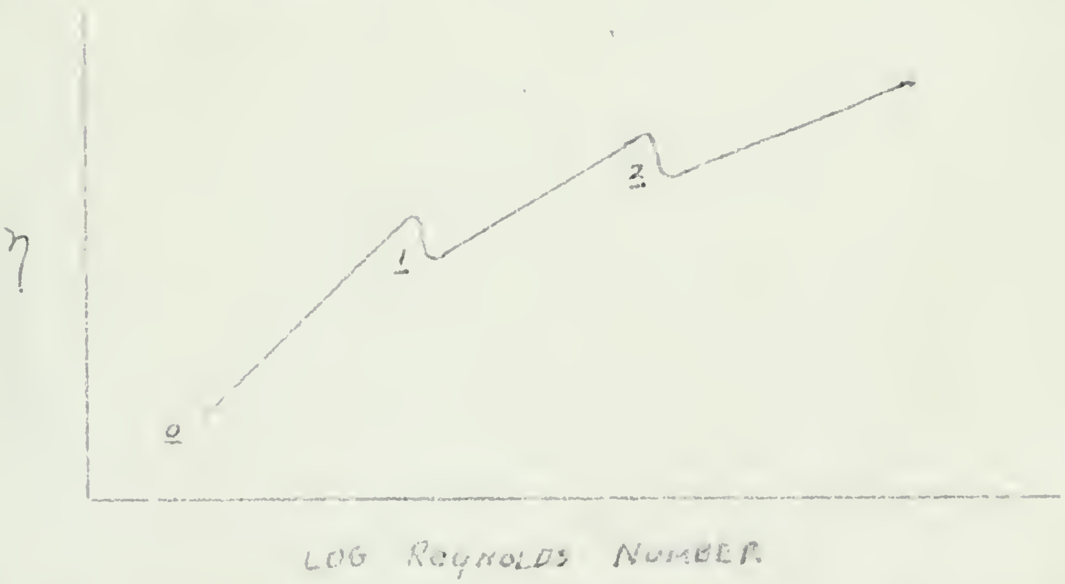

In the section from "0" to "1" laminar flow would be expected on both the convex and concave sides of the nozzle. At "1" transition to turbulent flow on the concave side occurs. At "2" transition occurs on the convex side and past "2" turbulent flow exists on both sides of the nozzle. The slope of the curve tends to decrease as Reynolds' Number increased. This is due to the nature of the friction versus Reynolds' Number curves. The side walls have not been considered in describing this ideal curve. Boundary

layer on the side walls will affect nozzle efficiency and may serve to complicate a curve drawn from test data. From curves similar to this previously drawn by the General Electric Company it is known that difficulty may be expected in determining and accurately plotting around the transition points.

In using the interferometer to measure the density gradients in the nozzle a steady state flow must first be reached. When the interferometer picture is interpreted, it must be borne in mind that the absolute densities and the density gradients are both integrated values taken across the depth of the picture, i.e., taken between the two side walls. This means that the density gradients existing next to the side walls will be superimposed on the density gradients existing in the nozzel, and as a result the true density at a particular point cannot be definitely established. It is hoped, however, that the interferometer will supply valuable information, particularly in regard to the boundary layer on the blade contours. Static pressure readings can be taken at the twenty-four pressure taps at the same time the picture is taken and they will undoubtedly help in evaluating the density gradients on the interferometer picture.

The exit flow from the nozzles may also be studied using the interferometer.

The traverse is made at the nozzles' exit with a total head tube of 0.059 inches outside diameter and it has been utilized in the pump side to check the apparatus that the interference of the flow past this tube is sufficient to cause fluctuations in the static pressure readings along the nozzle walls. These fluctuations appear pronounced to the first indication, but whether they are serious enough to necessitate a reduction in the tube diameter is not known yet.

The fluid flow in the nozzle can be expected to pile up towards the outside of the turn. This will cause the pressure to increase locally on the concave side of the blades. The velocity vectors will be reduced in magnitude from the average velocity and they will be inclined towards the concave side. This inclination of the velocity from the streamline direction carries over to the exit and is sometimes called "angle exaggeration" in the literature. These remarks are based on theoretical predictions, but early test results bear out this "angle exaggeration" at the exit.

RESULTS AND CONCLUSIONS

The primary accomplishment of this project was the design, construction, and installation of the model and its associated accessories. The project was undertaken with the understanding that as much as possible would be done, in the limited time available, toward the objectives of the sponsor. These objectives were to design, build, install

and test the nozzle partitions for the critical determination of nozzle efficiency as a function of both Reynolds' Number and Mach Number, and to use the interferometer to study thoroughly the effect of these variables on the general flow patterns and in particular the boundary layer. The total project will probably require about two more years to complete. It is regretted that the delays encountered prevented getting a good start on the actual testing of the model. Although the authors and sponsor feel that a major stride has been accomplished it would be a matter of personal satisfaction to have been able to work with the fruits of the labor. At any rate the model is now ready for testing.

(A) CALCULATION OF REYNOLDS NUMBER

$$Re = \frac{\rho V l}{\mu} = \frac{p_0}{R T_0} \times \frac{\rho}{\rho_0} \times \frac{V}{a} \times \frac{a}{a_0} \times \frac{l}{\mu} \times a_0$$

$$= \frac{p_0}{R T_0} \times \frac{\rho}{\rho_0} \times M \times \sqrt{\frac{T}{T_0}} \times \frac{l}{\mu} \times 49.1\sqrt{520}$$

Re = Reynolds number

ρ = density at nozzle exit

V = velocity at nozzle exit

A = speed of sound at nozzle exit

l = nozzle throat width = 0.5 inch

μ = viscosity of air = 12×10^{-6} lb/ft sec.

A_o = speed of sound where T_o = 520°R

T_o = total temperature at entrance = 520°R

P_o = total pressure at entrance

M = Mach number at exit

R = universal gas constant = 53.3 ft lb/lb°R

ρ_o = density of air corresponding to P_o and T_o

P = static pressure at exit

Table 30 of "Gas Tables" by Keenan and Kaye will be used.

For minimum Re; P_o = 1.0 psia, P/P_o = .9[illegible]

$$Re = \frac{1.0 \times 144}{53.3 \times 520} \times .[illegible] \times .30 \times .[illegible] \times \frac{1/24 \times 10^6}{12} \times 49.1\ [illegible]$$

= 3,750

For maximum Re; P_o = [illegible].4 psia, P/P_o = .53

$$Re = \frac{27.4 \times 144}{53.3 \times 520} \times 1120 \times \frac{10^6}{24 \times 12} \times .95 \times .80 \times .847$$

= 543,000

μ is here considered constant. Actually the temperature at the exit will vary and therefore μ will vary with the temperature.

(B) CALCULATION OF BAND SHIFTS ON INTERFEROGRAMS

$$\varepsilon = (\rho_{tunnel} - \rho_x)\ \frac{L}{\lambda}\ \frac{n-1}{\rho} \qquad \text{(A)}$$

ε = fringe shift in band widths

ρ_{tunnel} = air density ahead of nozzle = $\dfrac{P_o}{R \times 520^{\circ}}$

ρ_x = air density at point being evaluated

L = light path length = 6 inches

λ = wave length of light in a vacuum

= 5461 A° = .215 x 10^{-4} inches (mercury green light)

$\dfrac{n-1}{\rho}$ = specific refractivity = .0036380 ft^3/lb

for derivation of this equation see thesis by John L. Morton III entitled "Design of A Mach Type Optical Interferometer for measurement of Density in Supersonic Wind Tunnel" on file at M. I. T.

For minimum Band Shifts (P/P_o = .25; P_o = 1.0 psia)

ρ_{tunnel} = .0052 lb/ft^3

ρ_x = .9565 (.0052) lb/ft^3

$$\varepsilon = \frac{2.27}{10^4} \times \frac{6 \times 10^4}{.215} \times \frac{36.38}{10^4} = .230$$

For maximum number band shifts; $\dfrac{P}{P_o}$ = .30; P_o = 29.4

ρ_{tunnel} = .1530 lb/ft^3

ρ_x = .649 x .1530 lb/ft^3 = .0993

$$\varepsilon = \frac{5.37}{10^2} \times \frac{6 \times 10^4}{.215} \times \frac{36.38}{10^4} = 54.4$$

In using the interferometer two interferograms are made. One is made at a no-flow condition; the other is made at the flow condition in question. By superimposing one on top of the other on a light table the band shift, ϵ, at any point can be evaluated, and if the absolute density at some point in the interferogram is known, the absolute density at all points can be computed using equation [illegible].

C. DETERMINATION OF CURVES OF CONSTANT MACH NUMBERS ON A CHART OF NOZZLE EFFICIENCY VS REYNOLDS NUMBERS

The efficiency of the nozzle is defined as the ratio of the kinetic energy of the stream leaving the nozzle to the kinetic energy of a hypothetical stream leaving a reversible adiabatic nozzle which is supplied with the same kind of fluid in the same state and at the same velocity and which exhausts to the same pressure as the real nozzle.

The actual and theoretical kinetic energies of the stream leaving the nozzles are found by means of the impact pressures at the nozzle entrance and exit and the nozzle exhaust pressure. In accordance with the definition, the following procedure outlines the method of determining the nozzle efficiency for one point in the nozzle exit traverse.

$$\eta = \frac{h_{o2} - h_{2s}}{h_{o1} - h_{1s}} = \frac{T_{o2} - T_{2s}}{T_{o1} - T_{1s}} = \frac{1 - \frac{T_{2s}}{T_{o2}}}{1 - \frac{T_{1s}}{T_{o1}}}$$

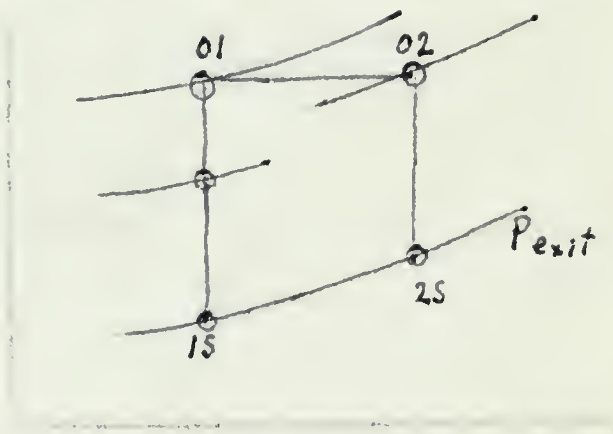

The nozzle is considered to be adiabatic and therefore T_{o1} equals T_{o2}. Entering the "One Dimensional Isentropic Compressible Flow Functions" table of Keenan-Kaye Gas Tables with the pressure ratios of static pressure at nozzle exit over total inlet pressure $\frac{p_e}{p_{o1}}$ and total exit pressure $\frac{p_e}{p_{o2}}$, the temperature ratios required for the determination of efficiency can be found.

During any one run, i.e., for any set Mach number and Reynolds number several total pressure readings must be recorded and the location of the point of each reading noted as the pitch distance is traversed. The efficiency for each point at which a pressure was recorded may then be computed. These point efficiencies can then be plotted on a graph of efficiency vs. distance along pitch line. The area under this curve divided by the pitch is then the integrated nozzle efficiency for that run. This then establishes one point on the chart of nozzle efficiency vs. Reynolds number. Since one of the objectives of the project is to obtain results which will allow one to differentiate between the effects of Mach number and Reynolds number, it is necessary to make several runs similar to the one described above, but at different Reynolds numbers, while holding Mach number at the same value. The results of these tests may then be plotted and a curve faired through the points. This now represents a curve of constant Mach number plotted on a chart of nozzle efficiency vs. Reynolds number. Repeating the procedure for several values of Mach number will yield a family of curves from which the separate effects of Mach number and Reynolds number upon nozzle efficiency may readily be determined.

Explanation of Runs Made 24 May 1949

All runs were made at a pressure ratio of .803; M = .59. This value was set arbitrarily.

$$\frac{P_{\text{static exit}}}{P_{\text{total ahead}}} = .803$$

Static pressure in the rectangular box ahead of the model varied from 9.14 psia to 15.14 psia. This does not represent the full range of the tunnel. Two more ejectors could have been cut in to further reduce the tunnel pressure. The upper limit was governed by the limits of the mercury manometer board. The difference in readings of total pressure ahead (with the pitot static tube) and total pressure behind (with the traverse) is quite small and a mercury manometer is not accurate enough for this purpose. The traverse was made at the centerline position, i.e., half way between the two side walls. Eleven positions of the traverse were used to cover the exit plane of the middle nozzle.

The exit flow angle is approximately 13°. The traverse is set 0.3 inches from the nozzle exit plane. Therefore, by simple calculation it can be shown that the traverse will be about 1.3 inches from a position directly over the trailing edge before the loss in total pressure of the flow next to the blade surface will be

indicated. This is shown on the curve of efficiency versus traverse position. It is expected that the efficiency of the middle position of the passage will be nearly 100%. The accuracy of these curves could be improved by taking more readings near the section where the losses are greatest.

The results are plotted as efficiency vs. Reynolds number (log Reynolds number was not used because of the small range of the test) for a constant Mach number of .59. As expected the curve shows an increase of efficiency with Reynolds number up to an apparent critical value where a dip in the curve shows a decrease in efficiency. The exact nature of this dip in the curve is uncertain due to the small number of test points in this range.

TEST DATA

For Runs made on May 24, 1949

Position	0.0	0.1	0.2	0.5	0.8	1.15	1.5	1.8	2.1	2.2	2.3
Static Exit	511.0	505.5	505.2	505.5	506.2	506.5	507.0	507.0	507.5	508.5	509.0
Total Entrance	418.5	413.0	4121	412.2	412.4	412.7	413.0	413.0	413.5	414.9	415.2
Total Exit	418.5	412.5	411.8	412.0	416.3	425.8	4150	414.3	414.5	416.0	416.5
Efficiecy	98.0	100	100	100	95.5	88.0	97.3	97.9	98.2	98.1	98.3

Static Exit	362.0	363.5	363.8	364.0	364.0	364.0	364.0	364.0	364.0	364.0	364.0
Total Entrance	233.2	233.8	234.0	233.9	233.8	233.9	233.9	233.9	233.9	233.9	234.0
Total Exit	232.1	233.9	234.0	234.0	241.8	245.8	234.2	234.2	234.3	234.2	234.2
Efficiency	100	100	100	100	94.2	92.0	99.8	99.8	99.8	100	100

Static Exit	325.3	325.5	326.0	326.0	326.0	326.2	326.3	326.3	326.3	326.3	326.3
Total Entrance	185.5	185.7	185.7	185.3	185.3	185.3	185.2	185.2	185.1	185.0	185.0
Total Exit	185.3	185.5	185.4	185.1	192.8	197.2	185.1	184.9	184.8	184.8	184.8
Efficiency	100	100	100	100	95.1	92.5	100	100	100	100	100

Static Exit	290.0	290.3	290.3	290.5	291.2	292.3	292.7	293.5	293.8	293.8	293.8
Total Entrance	139.8	139.5	139.1	138.9	139.7	140.3	140.5	141.0	141.2	141.3	141.3
Total Exit	139.8	139.1	139.0	138.8	148.8	143.8	143.3	141.4	141.6	141.7	141.7
Efficiency	100	100	100	100	95.0	98.1	99.4	99.8	100	100	100

Position indicates distance in inches behind blade trailing edge.

Pressures in millimeters of mercury. (Atmos. 126)

Position	0.0	0.1	0.2	0.5	0.8	1.15	1.5	1.8	2.1	2.2	2.2
Static Exit	268.3	268.5	268.5	268.7	269	269.5	270.0	270.0	270.0	270.0	270.0
Total Entrance	109.2	109.2	109.1	109.1	109.0	109.0	109.0	109.0	109.0	109.1	109.1
Total Exit	109.0	109.0	109.0	109.0	118.0	121.9	108.8	108.8	108.9	108.9	109.0
Efficiency	100	100	100	100	95.4	93.1	100	100	100	100	100
Static Exit	263.8	263.8	263.7	263.8	263.8	263.9	264.0	264.7	264.4	264.4	264.4
Total Entrance	103.8	103.8	103.8	103.8	103.7	103.0	103.8	103.6	103.8	103.8	103.8
Total Exit	103.3	103.5	103.3	103.3	112.5	116.4	103.0	103.0	103.0	103.1	103.0
Efficiency	100	100	100	100	96.3	92.7	100	100	100	100	100

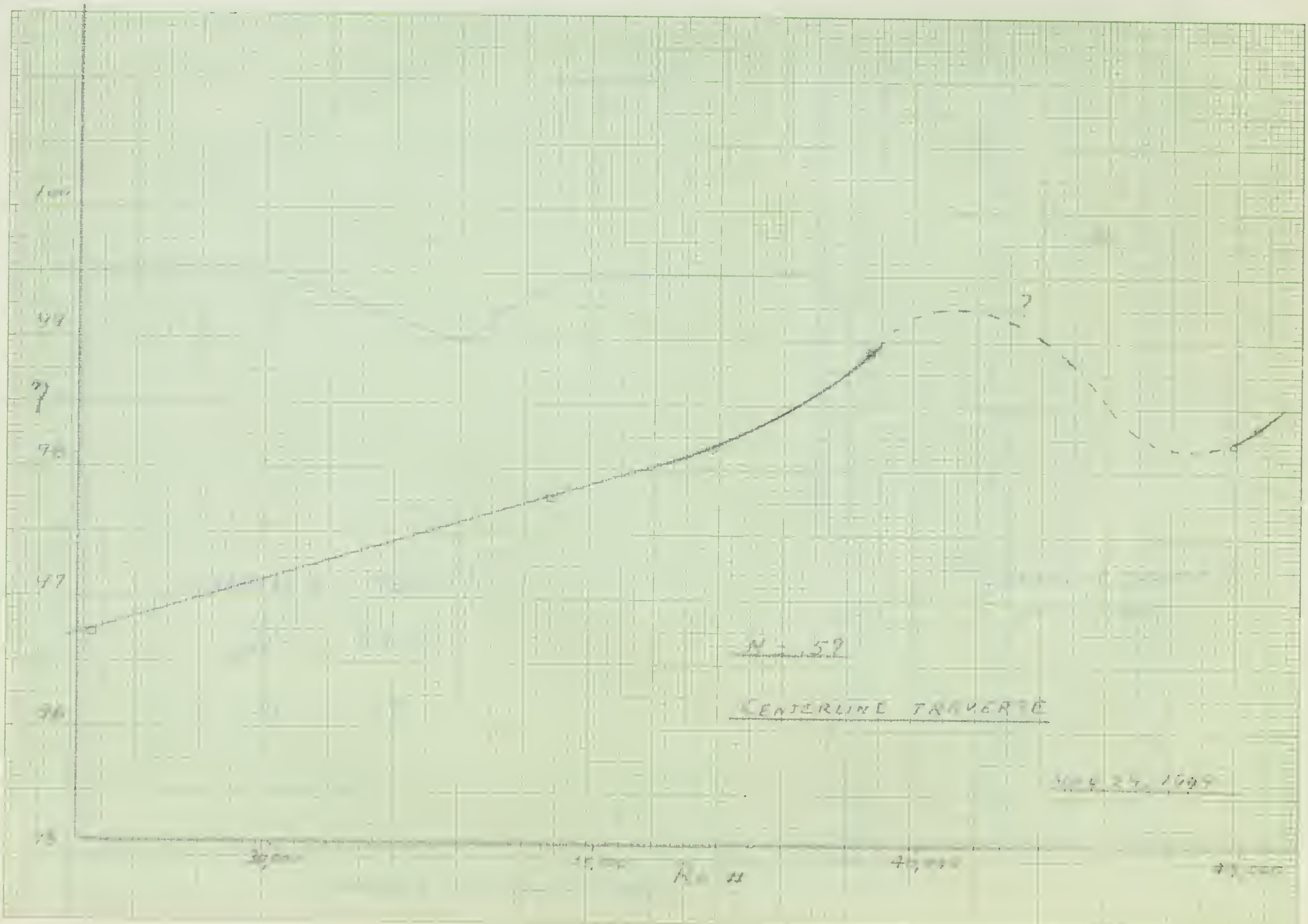

η
Re
CENTERLINE TRAVERSE

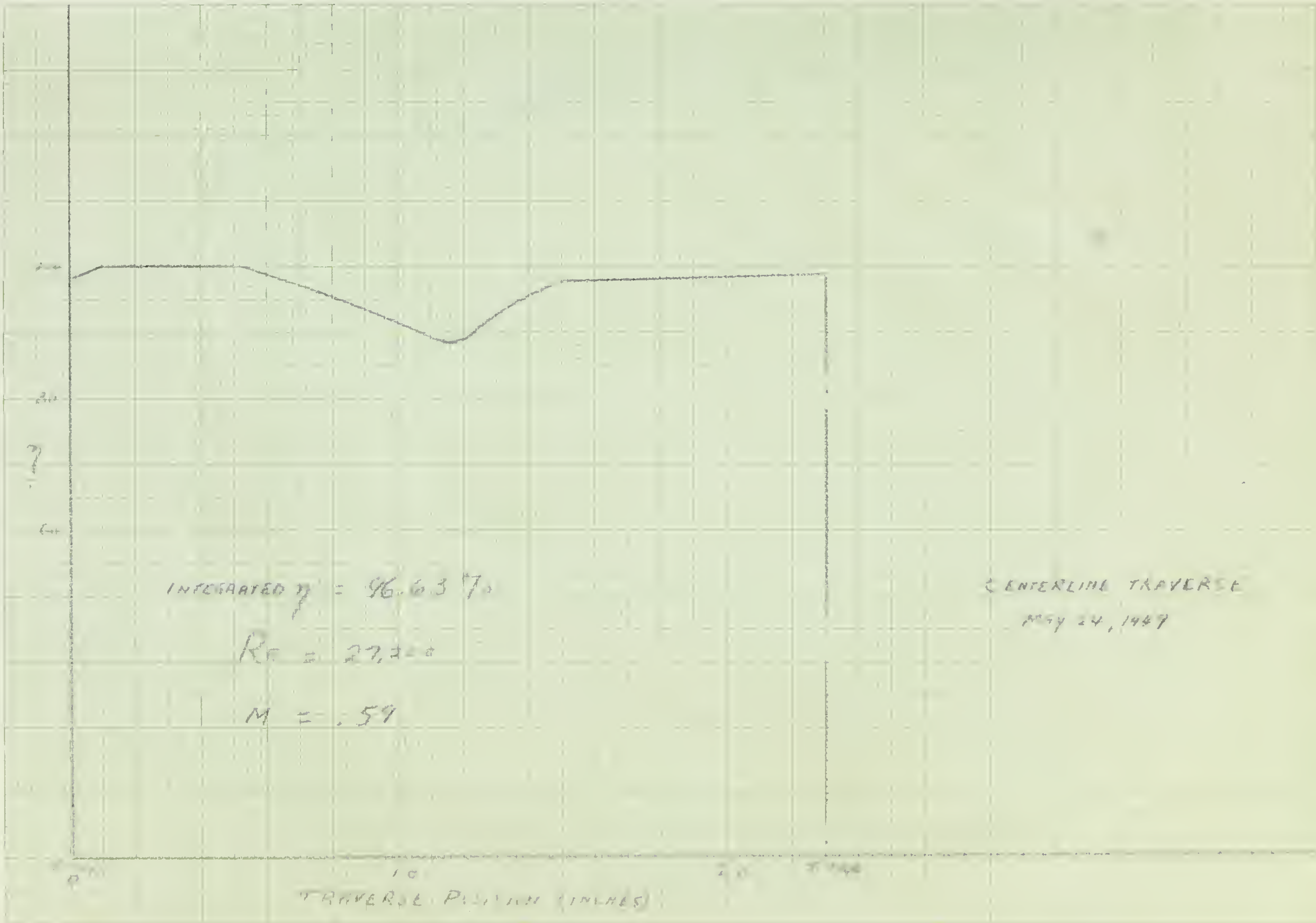
INTEGRATED η = 96.63 %
M = .59
CENTERLINE TRAVERSE

BIBLIOGRAPHY

1. "Design of a Mach-Type Optical Interferometer for Measurement of Density in a Supersonic Wind Tunnel" MIT thesis by John L. Norton III.

2. "Catalog of Performance Characteristics of Lattices" General Electric Report No. 31[illegible] by Hans Kraft.

3. "Development of, and Test Experience with "Battleship" Nozzle Partitions (K-6915609 and Similar)" General Electric Report No. 31966 by P. [illegible]. Moulton and R. Neal.

4. "Modern Developments in Fluid Dynamics" by S. Goldstein.

5. "The Design Development and Testing of Two-Dimensional Sharp Cornered Supersonic Nozzles" MIT thesis by Gilbert B. Edelman

6. "Thermodynamics" by Joseph H. Keenan

FIG. A

INTERFEROGRAM BAND SHIFTS EXPECTED FOR VARIOUS

REYNOLDS' NUMBERS AND PRESSURE RATIOS

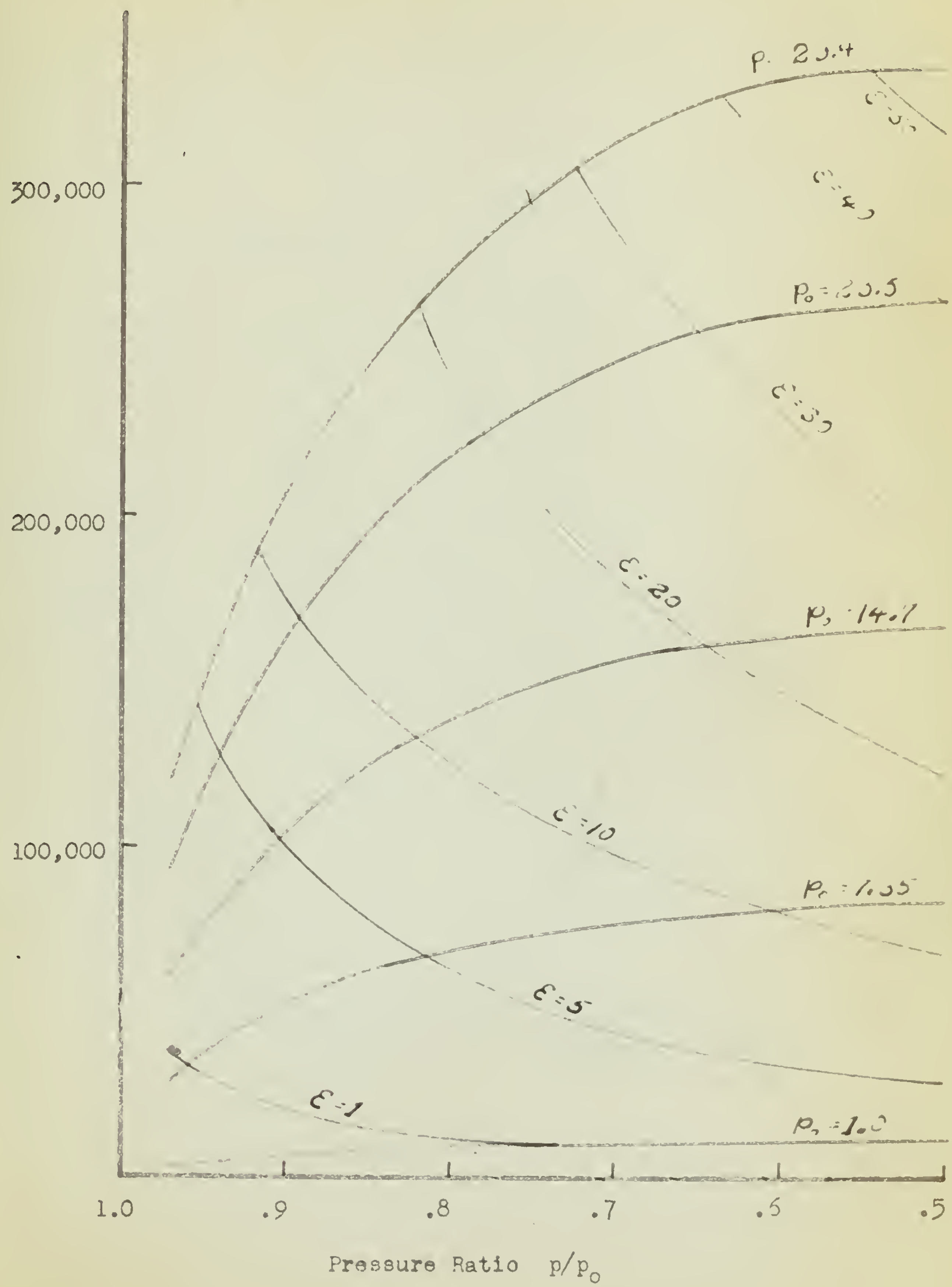

FIG. B

EXPECTED PERFORMANCE OF WIND TUNNEL COMPRESSORS

$$W = A \times \frac{p_0}{\sqrt{T_0}} \sqrt{\frac{2}{k-1}\left[\left(\frac{p}{p_0}\right)^{2/k} - \left(\frac{p}{p_0}\right)^{\frac{k+1}{k}}\right]}$$

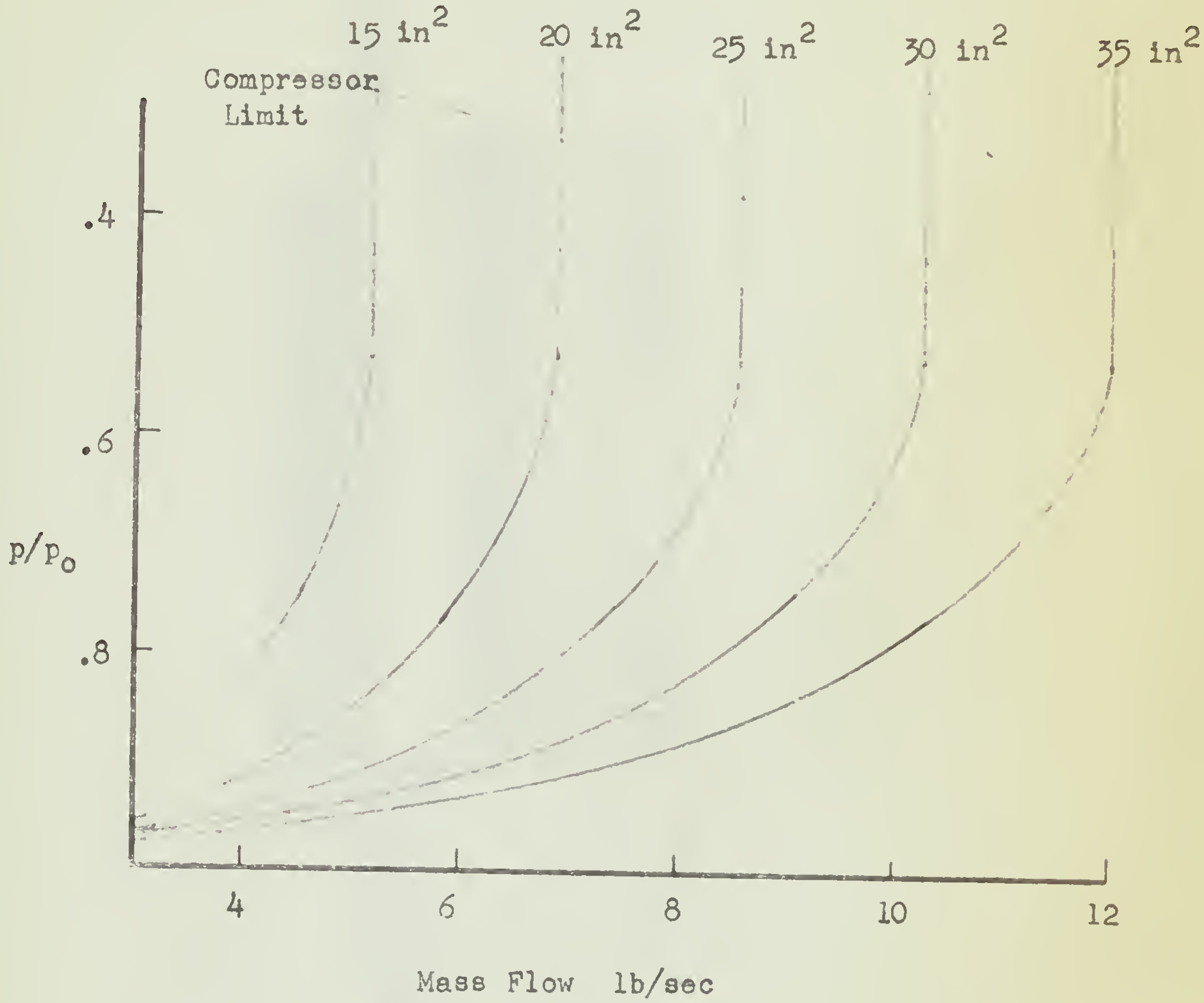

$$p/p_o = \frac{\text{Nozzle Exhaust}}{\text{Nozzle Inlet}} = \frac{\text{Compressor Inlet}}{\text{Compressor Exhaust}}$$

FIG. C

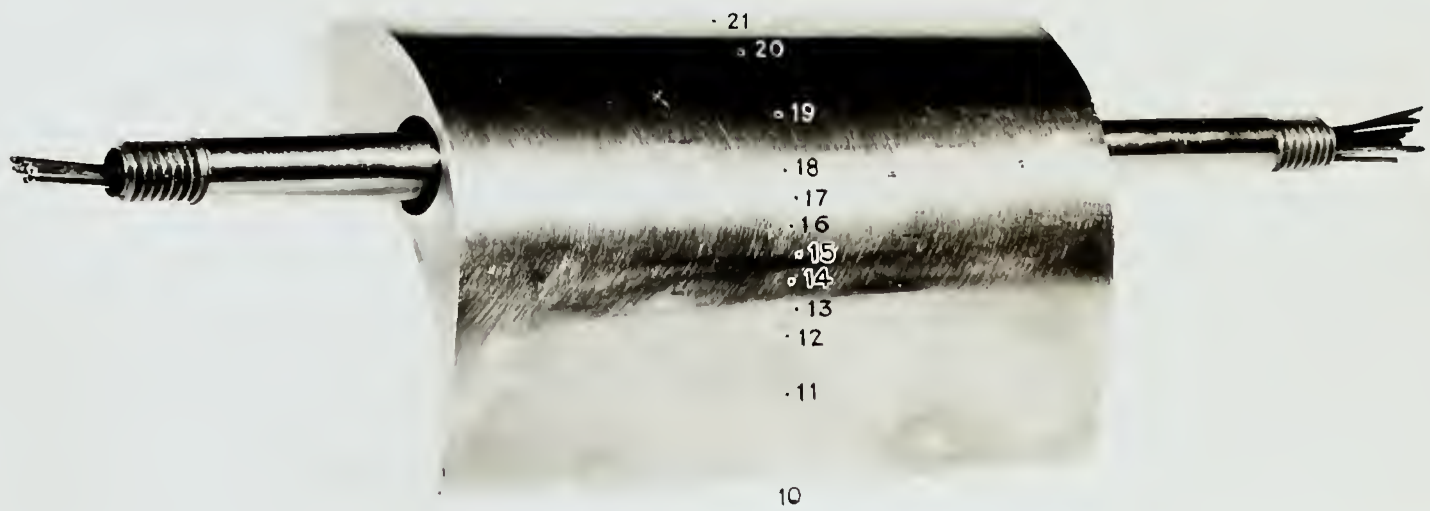

1067 290 PARTITION SECTIONS (TWICE SIZE BATTLESHIP K-6915600) WITH STATIC TAPS. FOR INTERFEROMETER MODEL T-9672723.

E329 4-8-49

FIG. D

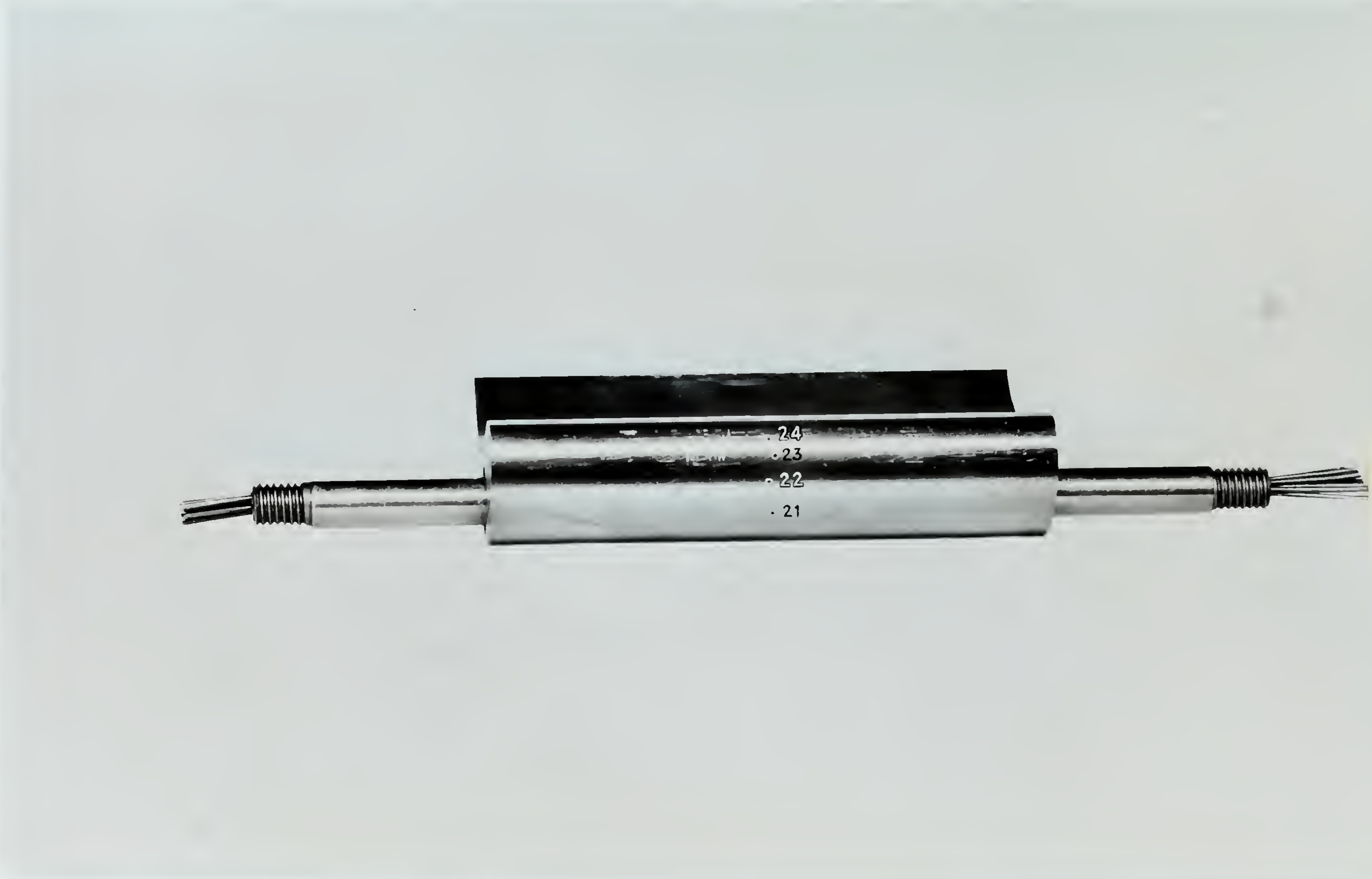

1067 288 PARTITION SECTIONS (TWICE SIZE BATTLESHIP K-6915600) WITH STATIC TAPS. FOR INTERFEROMETER MODEL T-9672723.

E329

4-8-49

FIG. E

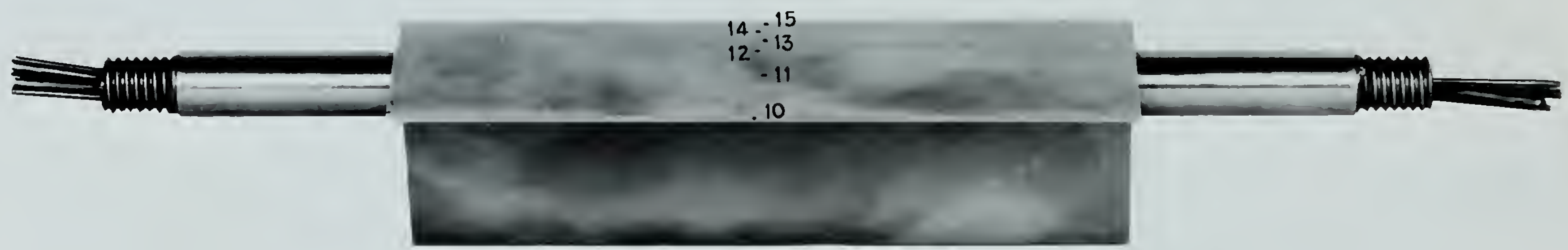

1067 289 PARTITION SECTIONS (TWICE SIZE BATTLESHIP K-6915600) WITH STATIC TAPS. FOR INTERFEROMETER MODEL T-9672723.

E329 4-8-49

FIG. F

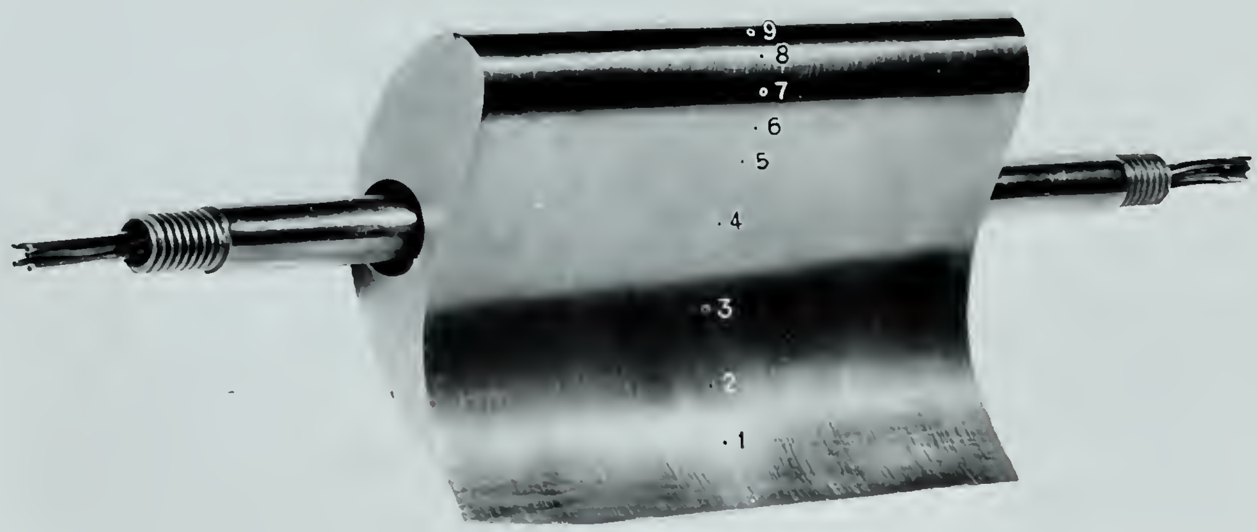

1067 292 PARTITION SECTIONS (TWICE SIZE BATTLESHIP K-6915600) WITH STATIC TAPS. FOR INTERFEROMETER MODEL T-9672723.

E329

4-8-49

FIG. G

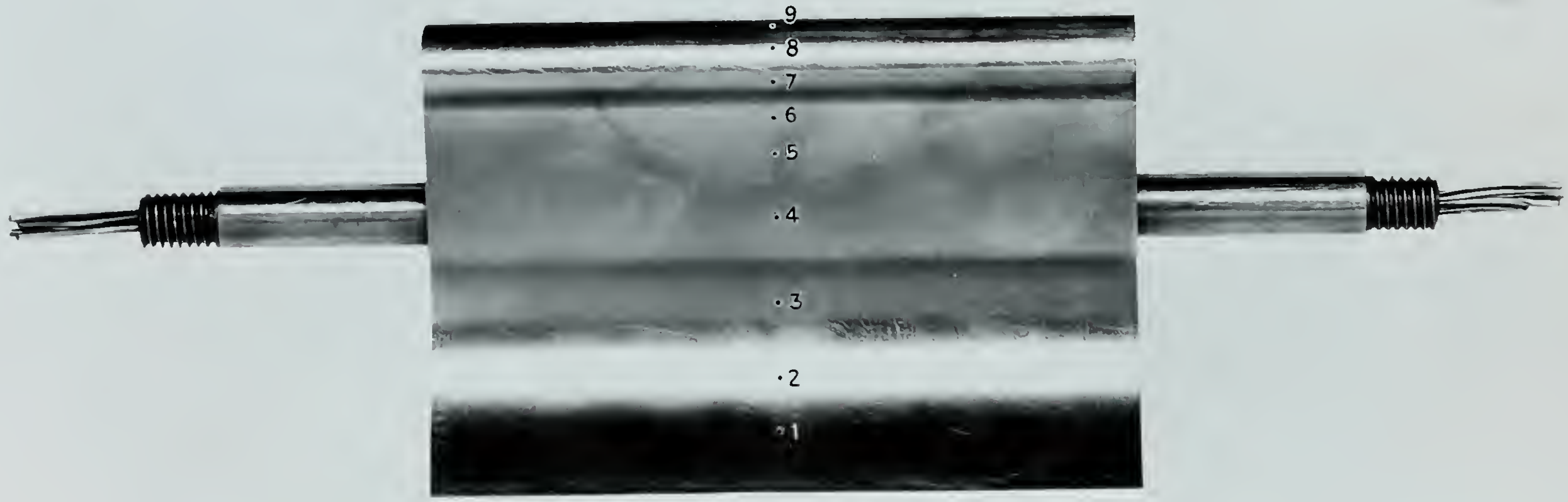

1067 291 PARTITION SECTIONS (TWICE SIZE BATTLESHIP K-6915600) WITH STATIC TAPS. FOR INTERFEROMETER MODEL T-9672723.

E329 4-8-49

FIG. H

1067 363 MODEL (DRAWING NO. T-9672723) FOR INTERFEROMETER INVESTIGATION OF TWICE SIZE OF BATTLESHIP PARTITION DRAWING NO. K-6915600.

E329 670

4-12-49

FIG. I

1067 364 MODEL (DRAWING NO. T-9672723) FOR INTERFEROMETER INVESTIGATION OF TWICE SIZE OF BATTLESHIP PARTITION DRAWING NO. K-6915600.

E329 670 4-12-49

FIG. J

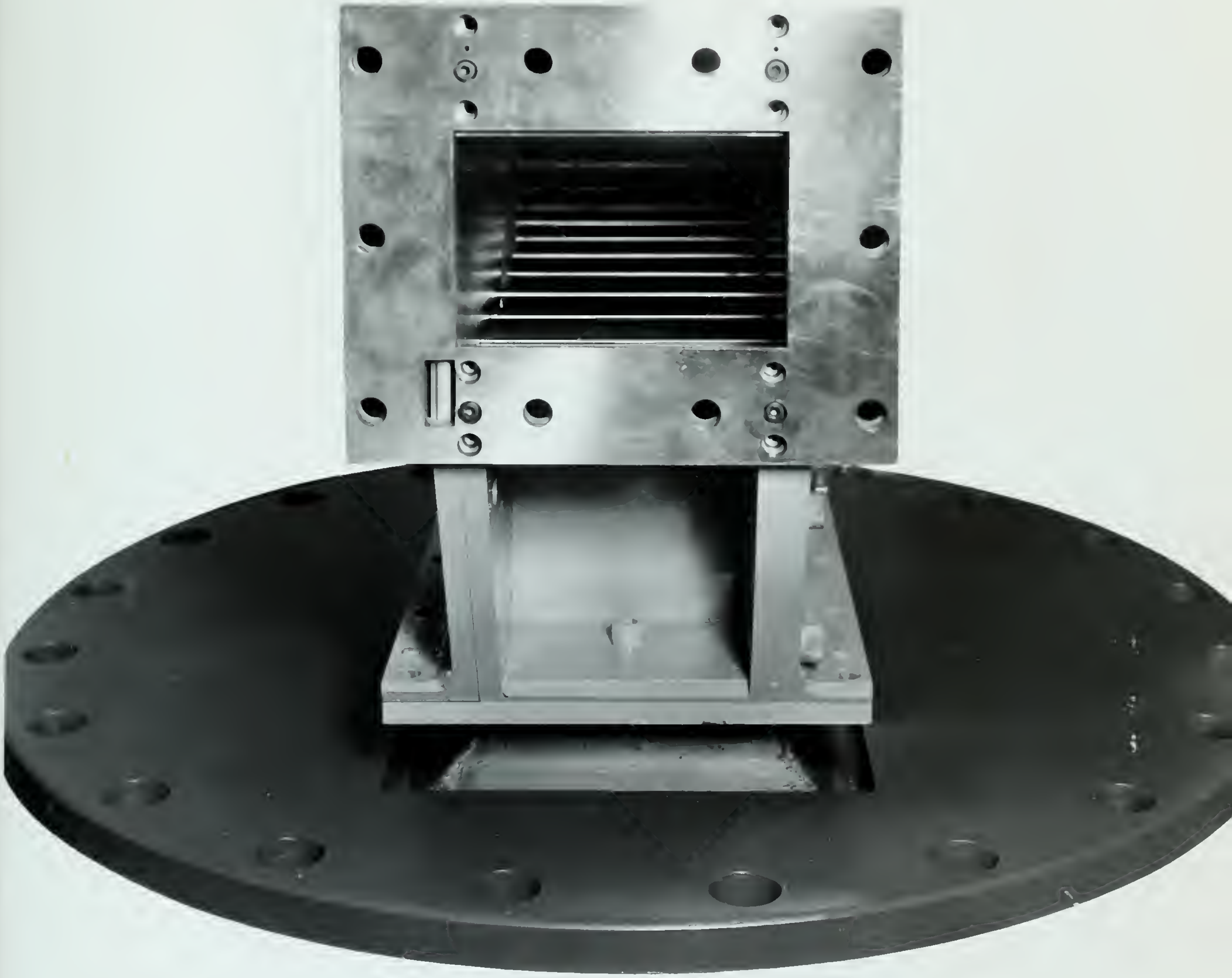

1067 367 MODEL (DRAWING NO. T-9672723) FOR INTERFEROMETER INVESTIGATION OF TWICE SIZE OF BATTLESHIP PARTITION DRAWING NO. K-6915600.

E329 670 4-12-49

FIG. K

1067 365 MODEL (DRAWING NO. T-9672723) FOR INTERFEROMETER INVESTIGATION OF TWICE SIZE OF BATTLESHIP PARTITION DRAWING NO. K-6915600.

E329 670

4-12-49

FIG. L

1067 362 MODEL (DRAWING NO. T-9672723) FOR INTERFEROMETER INVESTIGATION OF TWICE SIZE OF BATTLESHIP PARTITION DRAWING NO. K-6915600.

E323 670

4-12-49

FIG. M

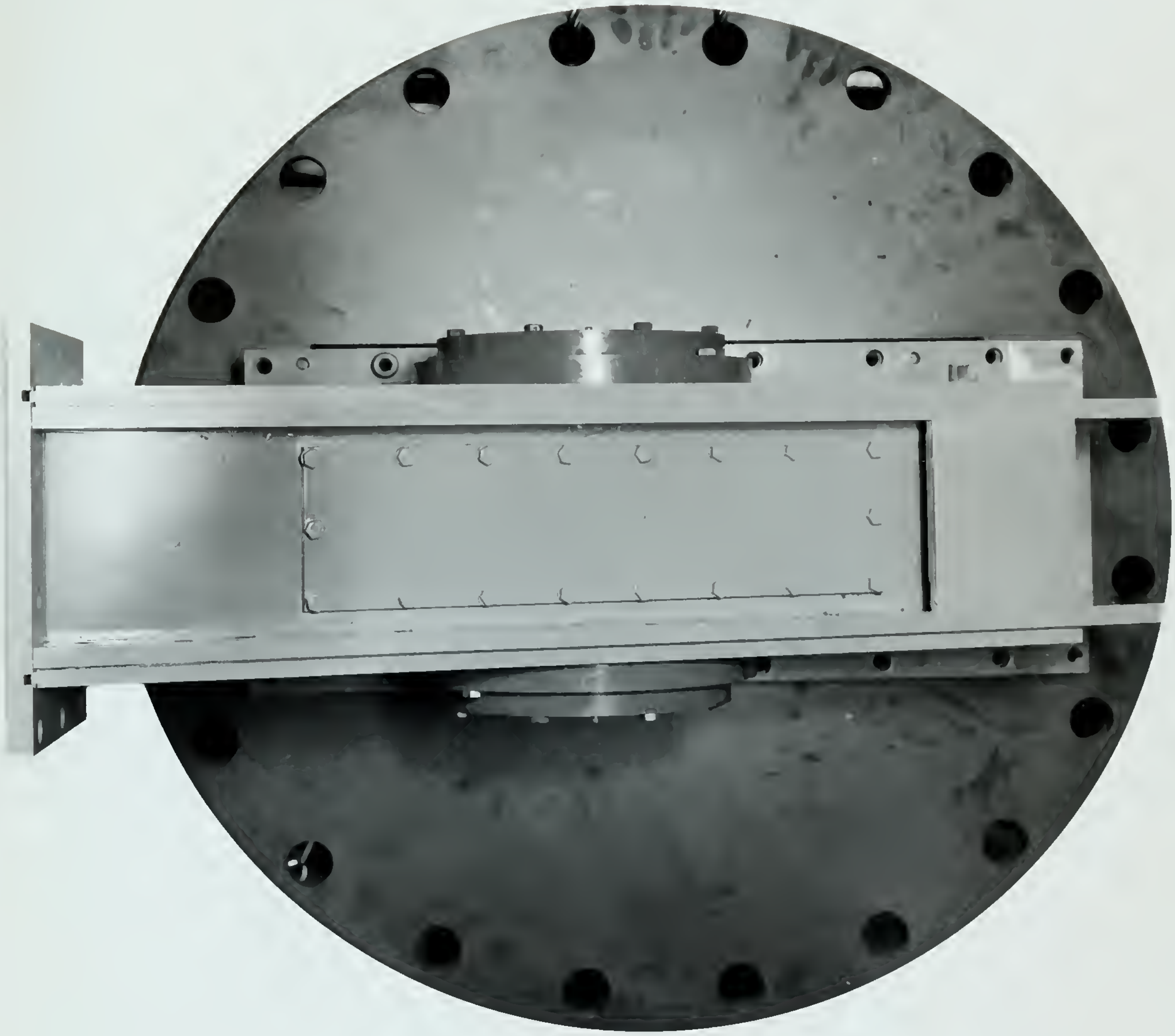

1067 366 MODEL (DRAWING NO. T-9672723) FOR INTERFEROMETER INVESTIGATION OF TWICE SIZE OF BATTLESHIP PARTITION DRAWING NO. K-6915600.

E329 670

4-12-49

FIG. N

MODEL INSTALLED - SHOWING TRAVERSING ASSEMBLY

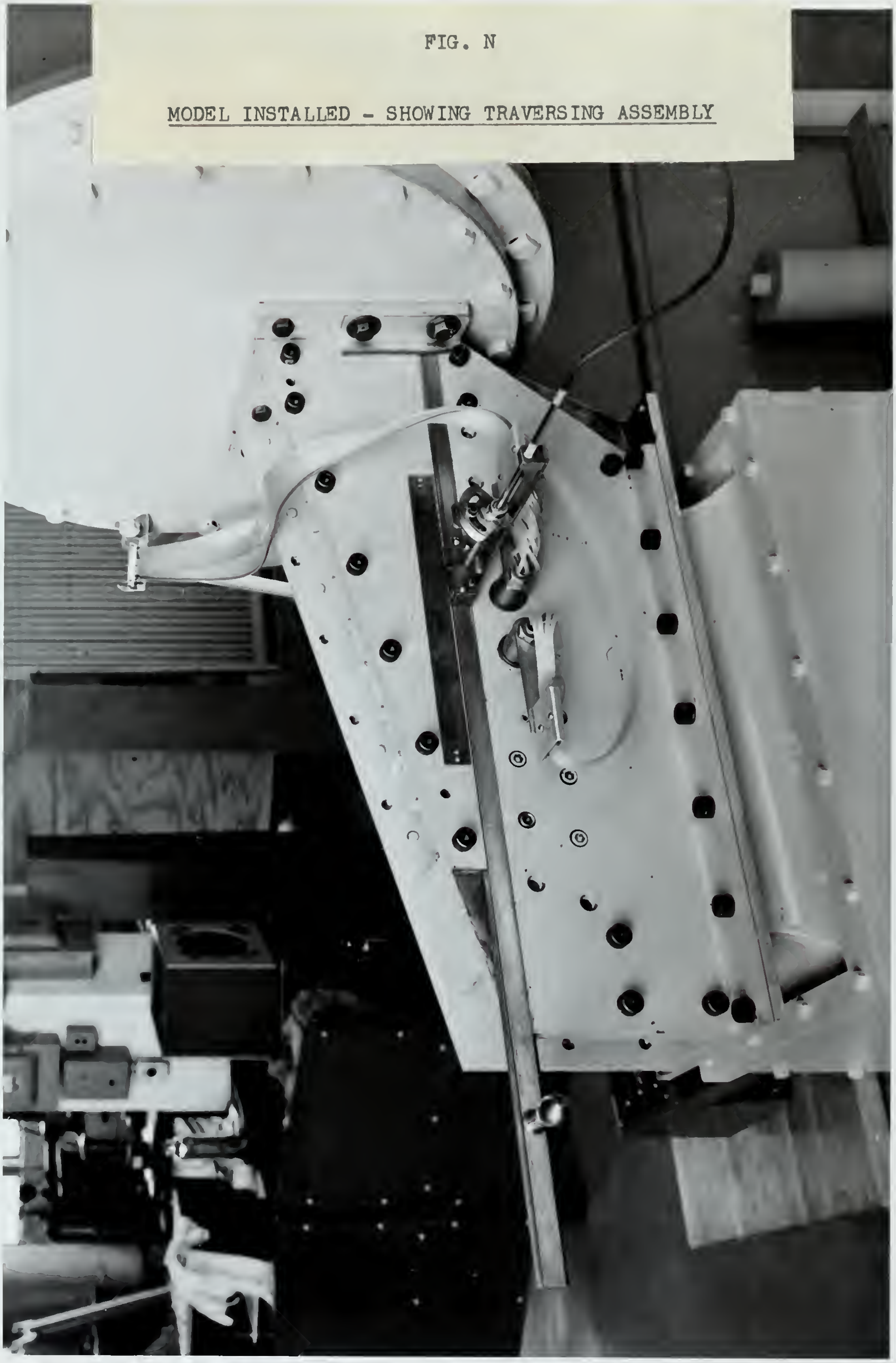

FIG. 0

MODEL INSTALLED - GENERAL ARRANGMENT

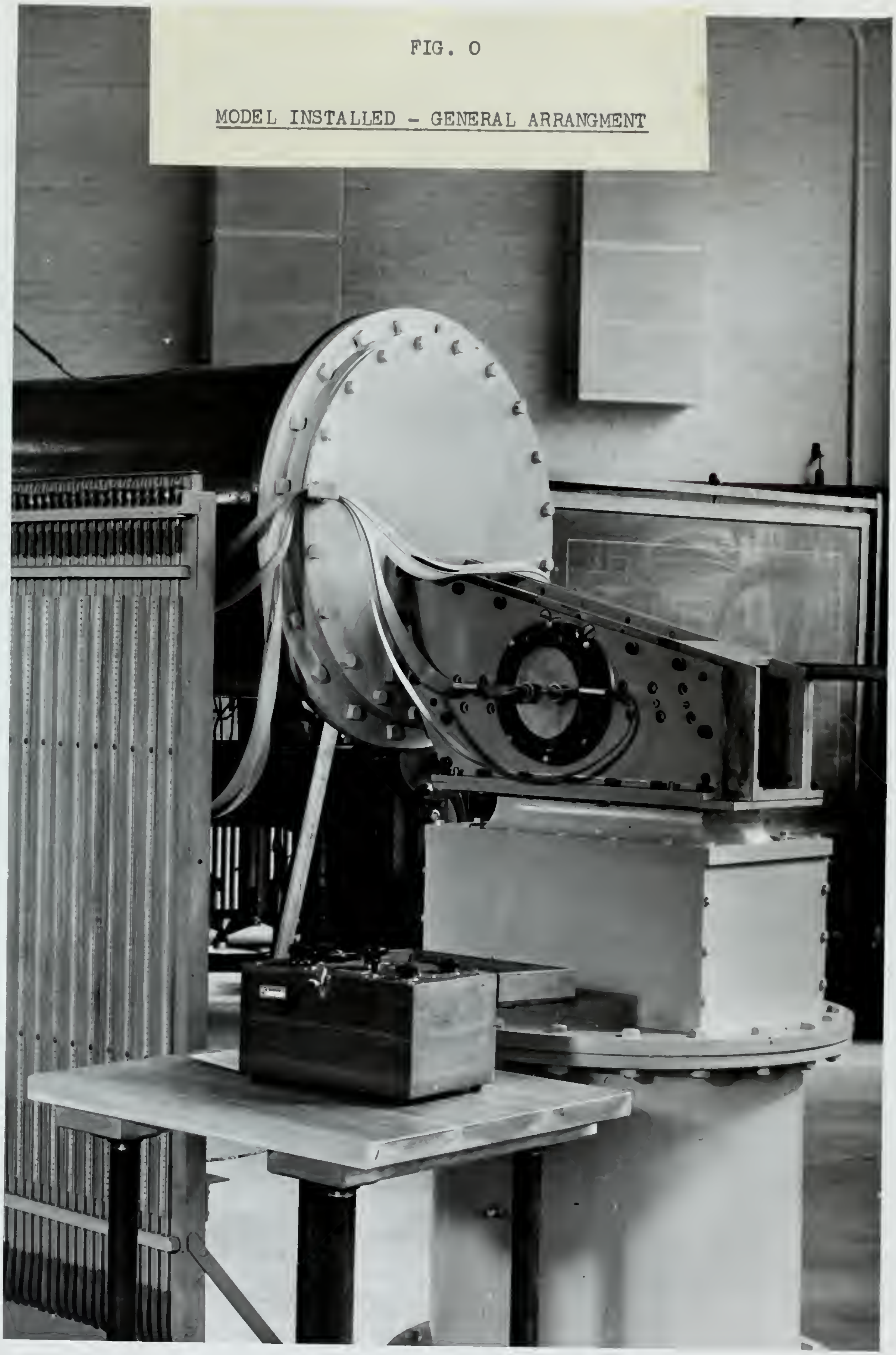


FIG. P
AIR SCREEN

FIG. Q

BLADE PROFILE

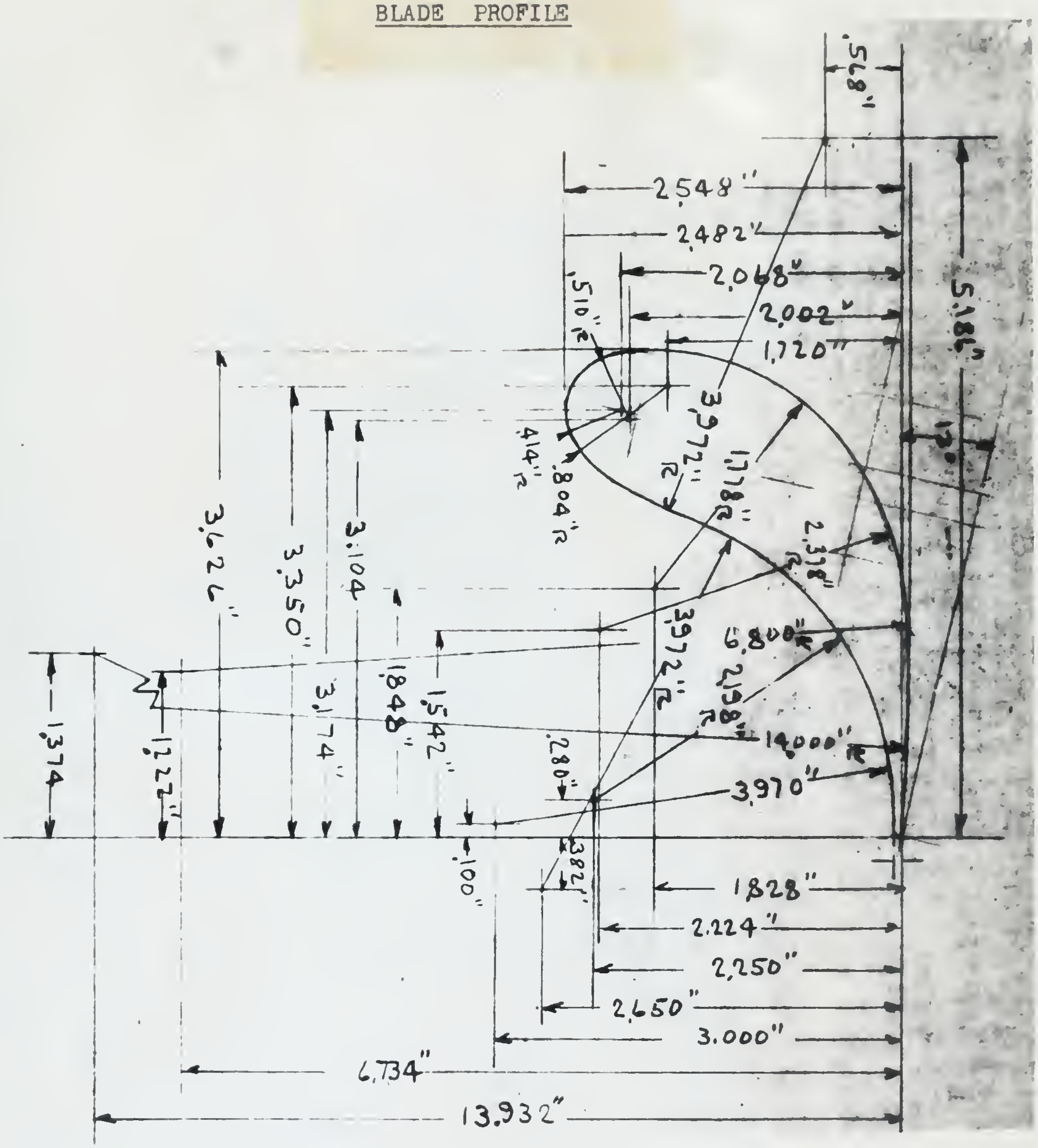

FIG. R

LOCATION OF PRESSURE TAPS

FORWARD BLADE

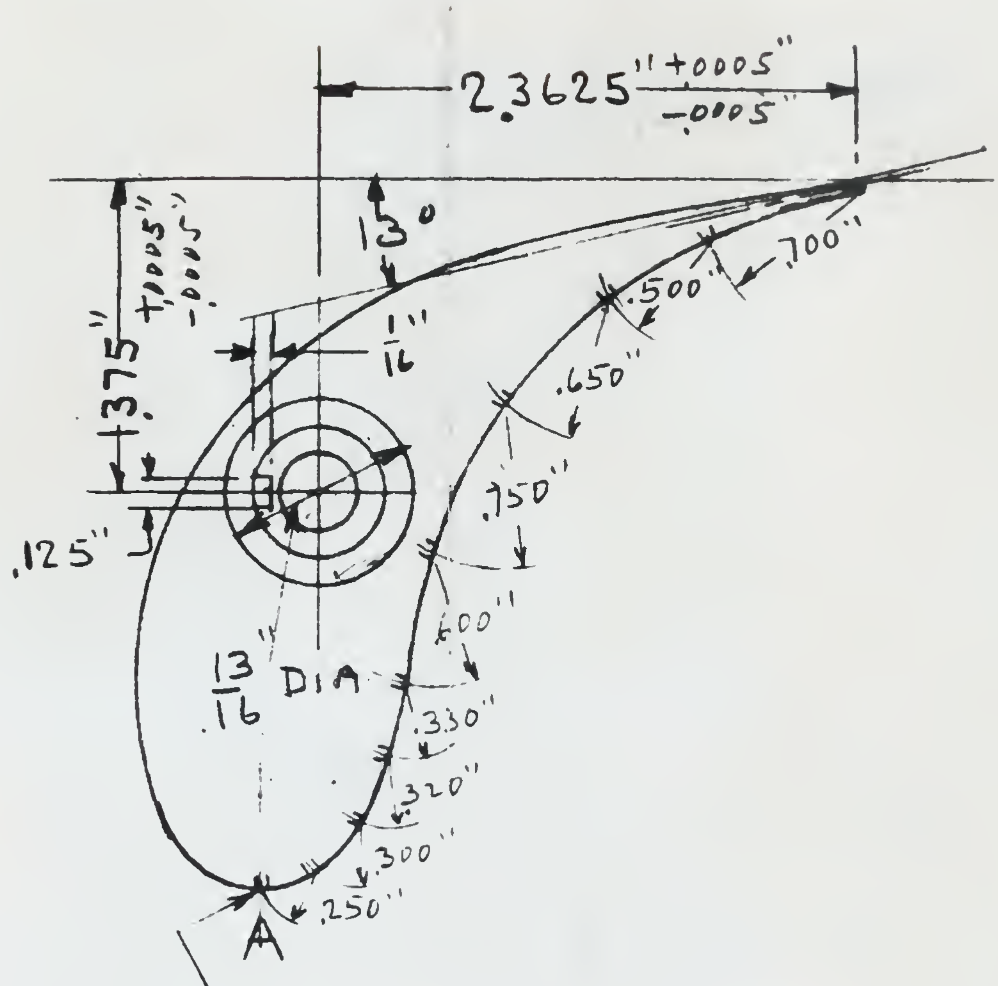

FIG. 8

LOCATION OF PRESSURE TAPS

REAR BLADE

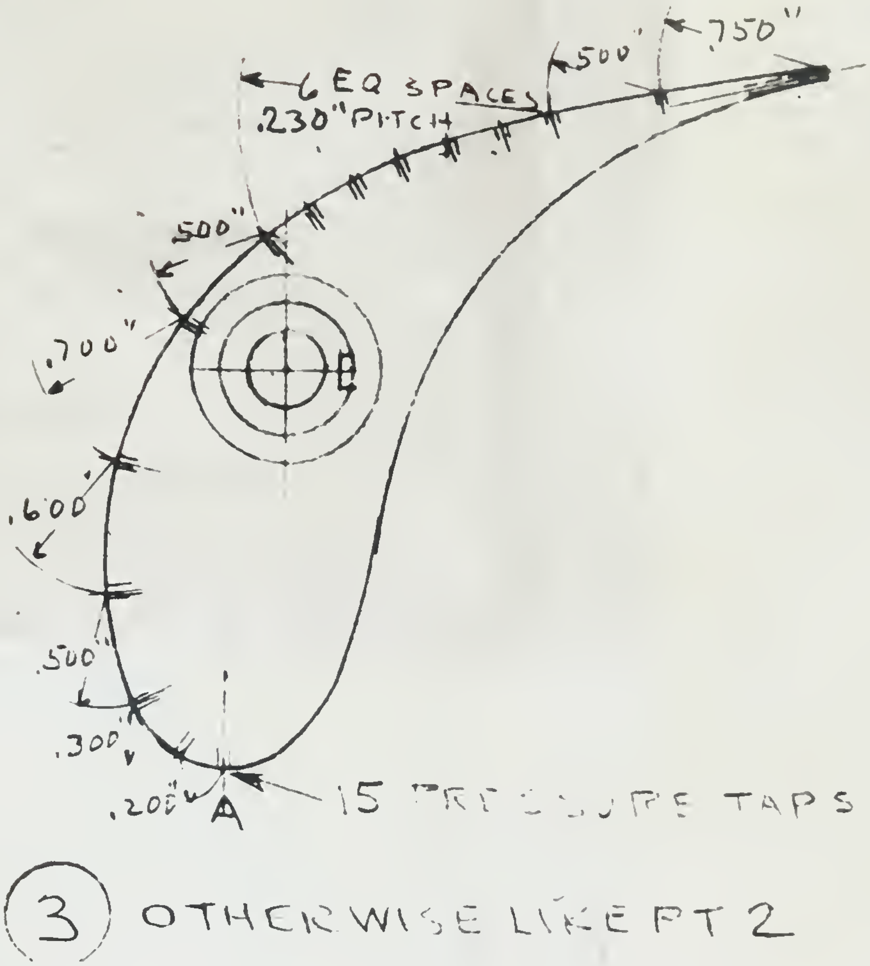

Thesis
B62
13665
Boettcher
The design, construction, and installation of a test model for the study of flow in nozzles.

Library
U. S. Naval Postgraduate School
Monterey, California